CHARACTERIZATION OF THE DAMPING PROPERTIES OF HIGH-DAMPING ALLOYS

by

I.G. Ritchie* and Z-L. Pan

ABSTRACT

Many problems of noise and vibration reduction cannot be solved by traditional methods using mechanical dampers or high-damping viscoelastic materials (e.g., rubbers, polymers and plastics). Often constraints imposed by the service environment, particularly those of stress, temperature and corrosive atmospheres, will force the design engineer to consider high-damping metals, alloys and composite materials. Unfortunately, characterization of the damping and stiffness properties of promising high damping metals and alloys has hardly ever been carried out in a systematic manner. Consequently, damping data are rarely accessible to the design engineer in a readily usable form. This lack of standard data has resulted in relatively few cases where metals and alloys have been chosen specifically for their high-damping properties.

This paper outlines techniques and strategies to characterize the damping properties of high-damping metals and alloys that owe their damping behaviour to the major classes of high-damping mechanisms. The main goal of the characterization is to present the damping data in a form that can be readily used by the design engineer to predict the vibration response of a component fabricated from the high-damping metal or alloy in question.

*Materials and Mechanics Branch
AECL Research
Whiteshell Laboratories
PINAWA, Manitoba Canada ROE 1LO
(204) 753-2311

INTRODUCTION

Most of the comforts and conveniences of modern life include a penalty - some sort of pollution of the environment. It is fashionable to discuss atmospheric pollution, the degradation of the ozone layer and the "greenhouse effect" since the media maintain these problems in focus for the public. It is much less fashionable to discuss noise pollution and the health hazards of high levels of vibration. Nevertheless, levels of noise and vibration are becoming intolerable in many situations including the workplace, public transportation systems, and our homes. Even moderate levels of noise and vibration increase the stress of modern living. More importantly, continual exposure to high levels of noise and vibration can and does lead to serious health problems, ranging from industrial deafness to "white hand" disease, or Reynaud's syndrome. The former is one of the hazards of the workplace in many manufacturing and heavy industries; the latter is common to operators of power tools ranging from drills to chainsaws. Besides the obvious suffering of the victims in question, there are two other penalties involved: a drain on available health-care resources and a direct financial penalty to the employers through worker compensation payments. Added to the growing demand of the public for a better environment, the two penalties combine to form a powerful tool to reduce both noise and vibration.

Nowhere are the twin aggravations of noise and vibration more evident to the public at large than in various forms of transportation, ranging from road vehicles to airplanes. Two methods of attacking the problems are available: reduction of the noise and vibration at the source and isolation of the source from the operator, passenger and bystander. In both cases high-damping structures and materials can and do play an important role in improved designs. By high-damping structures in this context we mean suspensions for both the engine in its compartment and the vehicle as a whole. These suspensions involve springs and dashpots (shock absorbers); locally, the functions of both the springs and dashpots are often combined to a certain extent in a high-damping material, for example, in a rubber or polymer grommet or bushing. Such high-damping viscoelastic materials, used as dampers or vibration isolators, are very familiar to design engineers. Nevertheless, viscoelastic materials usually have several drawbacks that preclude their effective use in many technologically important situations. These include an intolerance to elevated temperatures and many corrosive atmospheres, as well as a limited load-bearing capacity. In many instances, the function of the high-damping viscoelastic material can be replaced by a high-damping metal, alloy or composite. Unfortunately, however, the documented uses of high-damping metals, alloys, multi-alloy laminates and metal-matrix composites are few and far between. Moreover, with a few outstanding exceptions, they tend to be rather exotic applications and confined to defense and aerospacial uses where cost is not the major concern. The most notable exception is grey cast iron - a composite material of graphite flakes in a steel matrix. This inexpensive high-damping material has long been used to reduce noise and vibration in applications as diverse as machine beds and brake rotors.

There are clear signs that the situation is changing. As the understanding of intrinsic damping mechanisms has increased, so has the list of available metals and alloys with high-damping properties. In fact,

enough progress has been made in the understanding of some high-damping mechanisms to design alloys specifically for high-damping properties. However, this progress is not matched by an appropriate increase in applications. There appears to be two main reasons for this lag: the complexity of intrinsic damping properties of metals and alloys and the lack of appropriate codes and standards for the testing of high-damping materials and for their incorporation into engineering structures.

The first of these problems can be overcome by the careful characterization of the damping properties of the metal or alloy in question, i.e., by the preparation of data sheets that allow the design engineer to read off the intrinsic damping of the material for any combination of the parameters that specify the service condition. The second is a problem for the standards agencies and will not be solved in the near future. However, these problems can be circumvented to a large extent by a substitution technique. Such a technique simply demonstrates the improvements in noise and vibration suppression to be gained from replacing the original material of the component or structure in question with a high-damping metal or alloy of equivalent strength and adequate thermo-physical properties.

The purpose of this paper is to briefly outline attempts at the characterization of the damping and stiffness properties of two very different types of materials. The first is a series of die-cast zinc-aluminum (ZA) foundry alloys that show remarkable amplitude-independent damping behaviour over the range of temperature and frequency of interest in practical applications. The second is SONOSTON, a Mn-Cu-based alloy developed for quiet submarine propellers, that exhibits a marked amplitude dependence in its damping behaviour.

MATERIALS

ZA ALLOYS

The materials chosen for the characterization study and their composition ranges are given in Table 1. The A380 aluminum alloy, a known low-damping material and the grey cast iron a known high-damping material were included for comparison purposes. With the exception of the grey cast iron and the superplastic zinc (SPZ), all of the materials were obtained in the form of die-cast plates (15 cm x 7 cm) of two thicknesses, 3.3 mm and 1.27 mm. Samples were machined from these plates to test in the various types of apparatus employed in the study. Samples of the SPZ were obtained from wrought sheets of two thicknesses, 3.18 mm and 1.5 mm; samples of the grey cast iron were obtained from a large commercial casting.

SONOSTON

The material chosen for characterization was cut from one blade of a four-blade integral propeller provided by the Defence Research Establishment Atlantic, Halifax, Canada. Samples DR-1 and DR-4 were cut from the thick end (close to the stock) and the thin end, respectively, of the blade. Although the overall compositions of these samples were similar, the compositions of the dendrites and interdendritic regions were substantially different [1], reflecting the different cooling rates, in the two regions of

the blade after casting. The composition of the samples tested is also shown in Table 1.

TABLE 1--Composition ranges of the alloys investigated.

Alloy Designation	Composition (wt%)						
	Zn	Al	Cu	Mg	Si	Fe	C
A380 (SC84A)	3.0	remainder	3.0-4.0	0.1	7.5-9.5	1.3	-
#3 (AG40A)	remainder	3.5-4.3	0.25	0.02-0.05	-	0.1	-
ZA8	remainder	8.0-8.8	0.8-1.3	0.015-0.030	-	0.1	-
ZA12	remainder	10.5-11.5	0.5-1.25	0.015-0.030	-	0.075	-
SPZ (ZA22)	78	22	-	-	-	-	-
ZA27	remainder	25-28	2.0-2.5	0.010-0.020	-	0.010	-
Grey Cast Iron	-	-	-	-	-	96	4

SONOSTON	Mn	Cu	Al	Fe	Ni	C	Si
	55.2	38.3	4.36	3.16	1.42	0.095	0.07

TECHNIQUES

LOW FREQUENCIES (1-10 Hz)

Samples were machined from the as-received, as-cast materials into small rectangular prisms, typically 5 mm x 2.5 mm x 1.0 mm, for testing in a low-frequency, flexure pendulum. The pendulum used in this study as well as its electronic instrumentation is described in detail elsewhere [2].

INTERMEDIATE FREQUENCIES (10-5000 Hz)

Samples in the form of rectangular section bars of various lengths and thicknesses were machined from the as-received materials for testing in both fixed-free (cantilever) and free-free resonant bar equipment [3]. A detailed description of some of these techniques adapted to the narrower goal of the investigation of elastic moduli is given in reference 4.

ULTRASONIC FREQUENCIES (40 kHz and 120 kHz)

Samples in the form of square-section (3 mm x 3 mm) prisms, 60 mm in length, were machined from the as-received materials for testing by the

automated piezoelectric ultrasonic composite oscillator technique (APUCOT). The basic composite oscillator is of conventional, four-component design [3,5], whereas the electronic instrumentation has been automated and improved. The length of each sample tested by the APUCOT was reduced from the initial 60 mm to match the resonant frequency (40 kHz) of the quartz driver and gauge crystals.

DAMPING AND YOUNG'S MODULUS MEASUREMENTS

Our electronic systems are designed so that, regardless of the frequency of measurement, damping or internal friction (IF) can be measured by three separate methods, viz,

i) in free decay at resonance,
ii) at constant strain amplitude (ε) at resonance (using a closed-loop driver), or
iii) from the half-width of the resonance peak.

All three techniques yield the same results within experimental error, but method ii) is by far the most convenient for measurements of IF continuously as function of temperature (T). Using the pendulum technique, only changes in the resonant frequency (f), where f^2 is proportional to Young's modulus (E), are easily measured. In contrast, using both the resonant bar techniques and the APUCOT, precise values of E as well as changes in E can be monitored.

The measure of damping or IF used in this study is Q^{-1}, while E is given in GPa and T in degrees Celsius. We consider a metal or alloy to be among the HIDAMETS (high-damping metals) when $Q^{-1} \geq 10^{-2}$.

EXPERIMENTAL STRATEGY

Because of the delicate way in which the samples must be supported at their nodal planes in free-free resonant bar experiments, it is difficult and time-consuming to monitor changes in IF over a wide range of ε or T. In contrast, both types of experiment are more easily accomplished using the flexure pendulum or the APUCOT. Consequently, our testing strategy for the characterization of the damping and stiffness of materials has been to concentrate on flexure pendulum measurements and APUCOT measurements to investigate the ε dependence and the T dependence of the IF in an attempt to identify the mechanisms involved, and from the results to produce a master expression for the IF as a function of frequency at constant T and ε. It is then possible to check the validity of the master expression, at intermediate frequencies and a few discrete temperatures, using the resonant bar techniques.

At the phenomenological level, most IF mechanisms can be split into three classes: dynamic hysteresis, static hysteresis, and mechanisms that combine aspects of both. Dynamic hysteresis yields damping that is amplitude-independent and frequency (or T)-dependent (Fig. 1(a)). Static hysteresis yields damping that is amplitude-dependent and frequency-independent (Fig. 1(b)). As we shall see in the following, the strategy outlined above worked well for the amplitude-independent ZA alloys, but not at all for the SONOSTON, which combines aspects of both dynamic and static hysteresis.

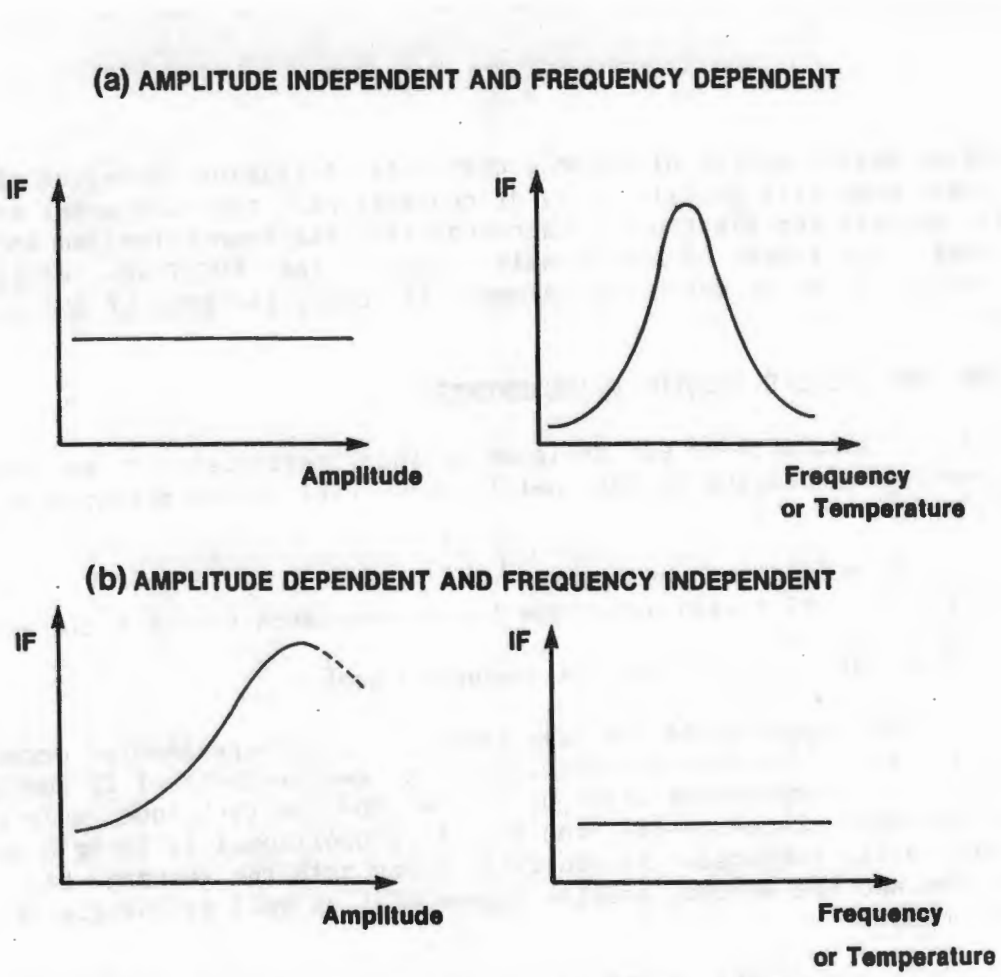

FIGURE 1: Schematic diagrams of internal friction as a function of strain amplitude for (a) amplitude-independent (dynamic hysteresis) and (b) amplitude-dependent (static hysteresis) damping.

RESULTS

ZA ALLOYS

The first flexure pendulum experiments (~4 Hz), on any one of the materials, using samples of two different thicknesses immediately revealed a strong dependence of the damping on the thickness in bending. This in turn suggested the existence of a large thermoelastic component, subsequently confirmed by the frequency dependence of the damping of samples of the same thickness and different lengths, and calculations of the thermoelastic damping using Zener's theory [6] and the known thermophysical properties of the materials (Fig.2). Other flexure pendulum measurements established the presence of a large peak as a function of T, culminating in a phase change at about 290°C, as shown in Fig. 3 for SPZ and ZA27. Low-frequency and high-frequency measurements of the low-temperature tail of this peak, as well as the strain amplitude dependence of the IF at ambient temperature (~20°C), are shown in Fig. 4 for ZA27.

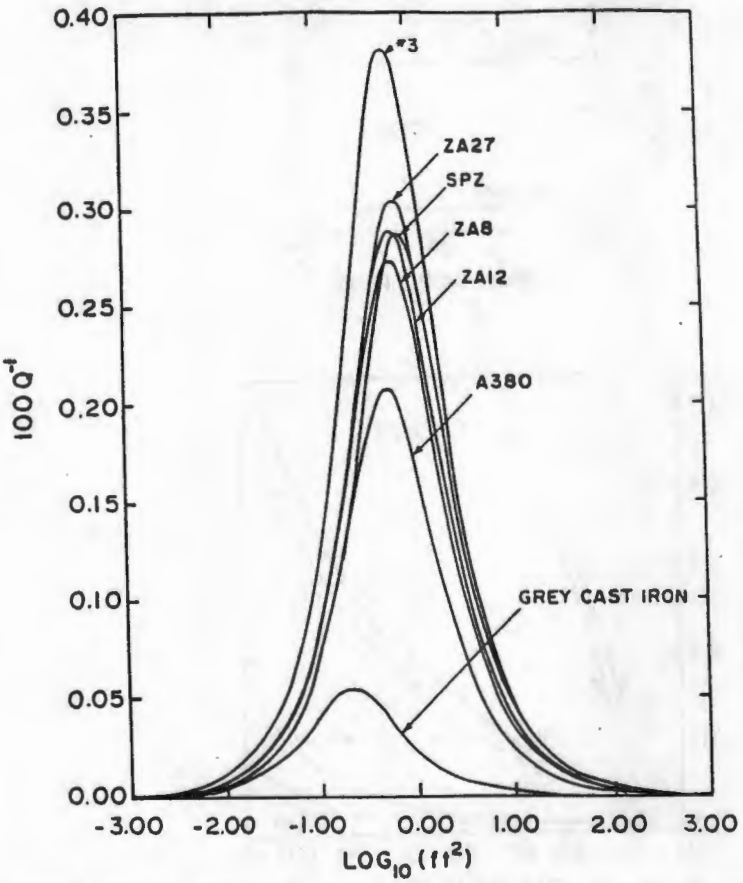

FIGURE 2: Thermoelastic damping peaks plotted as a function of $\log(ft^2)$, where f is the frequency in hertz and t is the specimen thickness in centimetres, for the ZA alloys, A380 and grey cast iron.

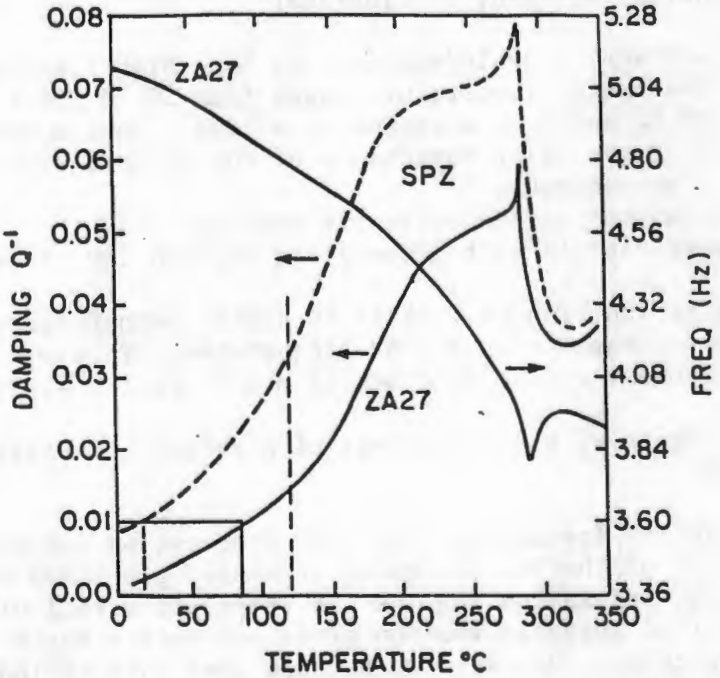

FIGURE 3: Damping, Q^{-1}, and resonant frequency (Hz) as a function of temperature for ZA27 and SPZ. The vertical dotted lines indicate the temperature range of practical interest.

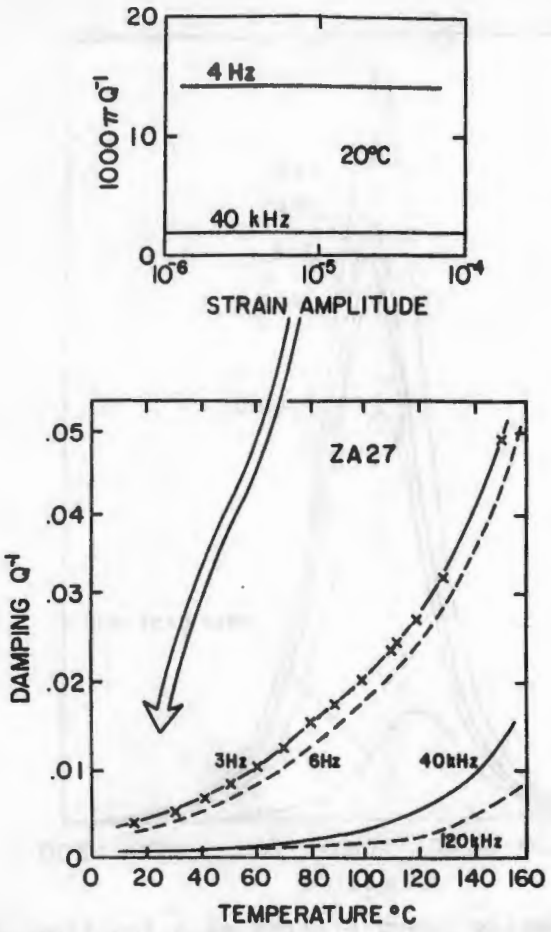

FIGURE 4: Damping, Q^{-1}, as a function of temperature and strain amplitude (at 20°C) for ZA27.

Combining the results of the flexure pendulum and the APUCOT measurements revealed the following important conclusions:

1. The IF and E are amplitude-independent at both high frequencies and low frequencies over the useful temperature range from 20 to 150°C. Such purely linear behaviour of IF and E in a series of alloys is quite unusual and indicates that all of the major components of the IF come from linear, dynamic relaxation mechanisms.
2. One of the mechanisms is thermoelastic damping.
3. The IF increases rapidly with temperature at both low and high frequencies.
4. The IF curves as function of T shift to higher temperatures (without noticeable change in shape) with higher frequencies. This strongly suggests that the major component of the IF comes from a thermally activated relaxation.
5. These results agree with the findings of previous investigations into the SPZ alloy [7-9].

If the IF at both low frequencies and high frequencies can be accurately described by the sum of the two thermally activated processes mentioned above (thermoelastic relaxation and the low temperature tail of a boundary relaxation), then this suggests that no other mechanisms become active at intermediate frequencies. However, to be sure that this is indeed the case, data at the intermediate frequencies must be collected and they too should be described by the sum of the two components.

SEMI-EMPIRICAL DESCRIPTION OF THE IF

The main results of the IF study of the ZA alloys are most easily displayed in a log Q^{-1} vs. log F plot, as shown in Fig. 5 for ZA27. The scatter is somewhat large, but not unduly so considering that the samples were cut from commercial die castings with variations in porosity, composition and other microstructural characteristics. Also, it should be noted that each datum is the average of at least three repeat measurements on a separate sample of the same thickness. The IF is highly reproducible for repeat measurements on the same sample, but variable from sample to sample cut from the same die casting.

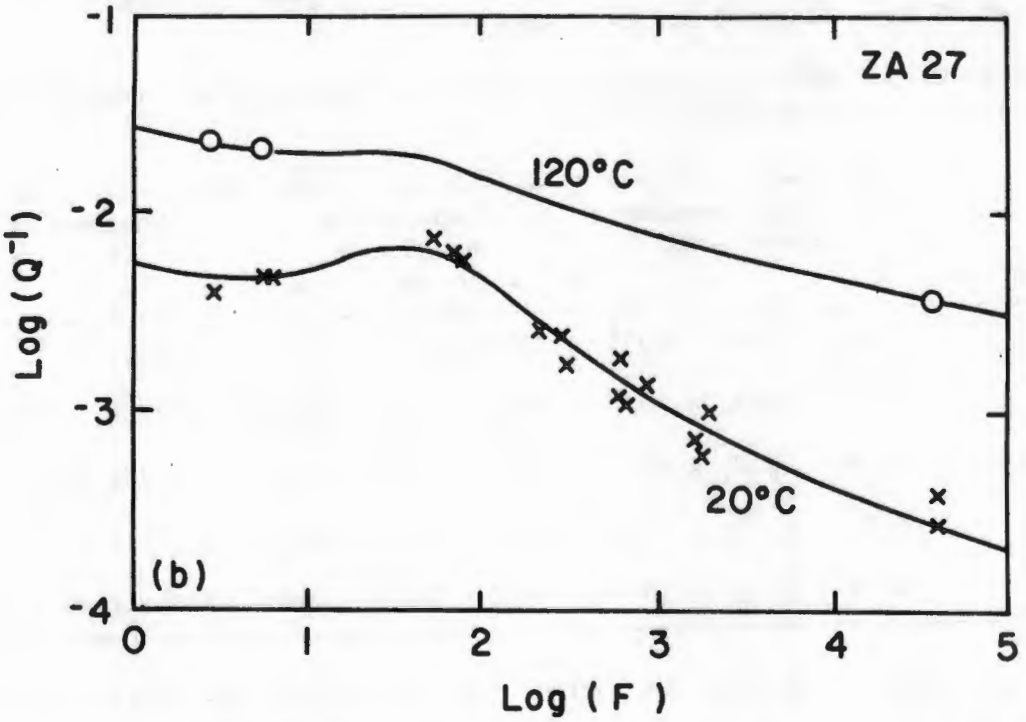

FIGURE 5: Log-log plot of damping Q^{-1}, as a function of frequency, f, for ZA27 at 20°C and 120°C. The full curves were calculated using equation (2) and the data in Table 2.

We expect to be able to describe the data of Fig.5 by an expression of the form

$$Q^{-1}(t,f,T) = \text{Background} + \frac{A}{f^n} \exp\left[\frac{-nH}{kT}\right] + \Delta_{TE}\omega\tau/[1 + (\omega\tau)^2] \qquad (1)$$

where $Q^{-1}(t,f,T)$ is the IF for a sample of thickness t, at frequency f and temperature T. In eqn. (1) the IF is given in terms of three components: (1) a temperature-independent background; (2) the tail of a broadened high-temperature peak, characterized by the exponent n, the activation enthalpy H, and the constant, A; and (3) the thermoelastic relaxation of strength, Δ_{TE}, and relaxation time τ. $\omega = 2\pi f$ is the radian frequency of the oscillations. Determination of n and H from the experimental results and

Δ_{TE} and τ from a combination of the thermophysical data on the alloys and the experimental results is described in detail in reference 10.

The experimental data obtained for all of the ZA series of alloys obtained over the temperature range from 20 to 150°C and the frequency range from 1 Hz to 120 kHz is well described by the semi-empirical formula derived from eqn. (1):

$$Q^{-1}(t,f,T) = \alpha_1 f^{-m} + \alpha_2 f^{-n}\exp(-\beta/T) + \alpha_3 T(ft^2)/[1 + (\delta_1 ft^2)^2] \qquad (2)$$

where the first term represents the f-dependent but T-independent background, the second term is the tail of a broadened high-temperature relaxation and the third term is the thermoelastic component. The constants for the various alloys are tabulated in Table 2. In Fig. 5 it is important to note that the calculated curve at 120°C is in good agreement with the limited IF data obtained at that temperature.

TABLE 2--Data used to describe the thickness, frequency and temperature dependence of the damping in the ZA alloys.

Material	Frequency-Dependent Background		Temperature Dependence			Thermoelastic Damping	
	m	α_1	α_2	n	β	α_3	δ
#3	0.26	$2.90_0 \times 10^{-3}$	5530	0.16	5222	3.963×10^{-5}	1.556
ZA8	0.28	$3.54_8 \times 10^{-3}$	4566	0.16	5106	2.758×10^{-5}	0.911
ZA12	0.29	$4.07_3 \times 10^{-3}$	2937	0.18	4758	2.863×10^{-5}	0.977
SPZ	0.22	$1.17_5 \times 10^{-2}$	16987	0.13	4875	2.335×10^{-5}	0.918
ZA27	0.29	$5.01_2 \times 10^{-3}$	6910	0.16	4990	5.016×10^{-5}	1.495

Young's modulus measured at ambient temperature for the ZA alloys is given in Table 3.

TABLE 3--Young's modulus of the ZA alloys measured at 20°C and 40 kHz.

Material	Young's Modulus (GPa)
≠3	93.8
ZA8	91.4
ZA12	89.5
SPZ	91.6
ZA27	78.0

SONOSTON

The IF of a sample of DR-1 as a function of ε at ambient temperature is shown in Fig. 6. Also, shown in Fig. 6 is the intrinsic IF of the material calculated from the specimen damping using the known strain distribution in the flexure pendulum sample. Details of this calculation are given elsewhere [11]. Similar experiments carried out on samples of both DR-1 and DR-4 using the APUCOT are shown in Fig. 7. Once again, the IF of the as-received SONOSTON is ε-dependent at high amplitudes, but the form of curves at 40 kHz are very different compared with those at low frequencies.

The IF and E as a function of temperature for a sample of DR-1 measured at about 4 Hz in the flexure pendulum and at about 40 kHz by APUCOT are compared in Fig. 8. The minima in f^2 (~4 Hz) and E (~40 kHz) mark the Néel temperature for the alloy. At temperatures below the minimum in E, the material is antiferromagnetic and the damping contains two components, an ε-dependent component and an ε-independent component. At temperatures higher than that of the minimum in E, the material is paramagnetic and the IF is ε-independent. This is borne out by the sets of Q^{-1} and E vs. T curves for different constant ε values shown in Figs. 9 and 10 for samples of DR-1 and DR-4 respectively. Fig. 8 also shows a rather complicated peak structure at low frequencies that shifts to higher temperature and increases in height at higher frequencies. A few tests at intermediate frequencies confirmed this observation. The sharp side or truncation of the high-frequency peak in

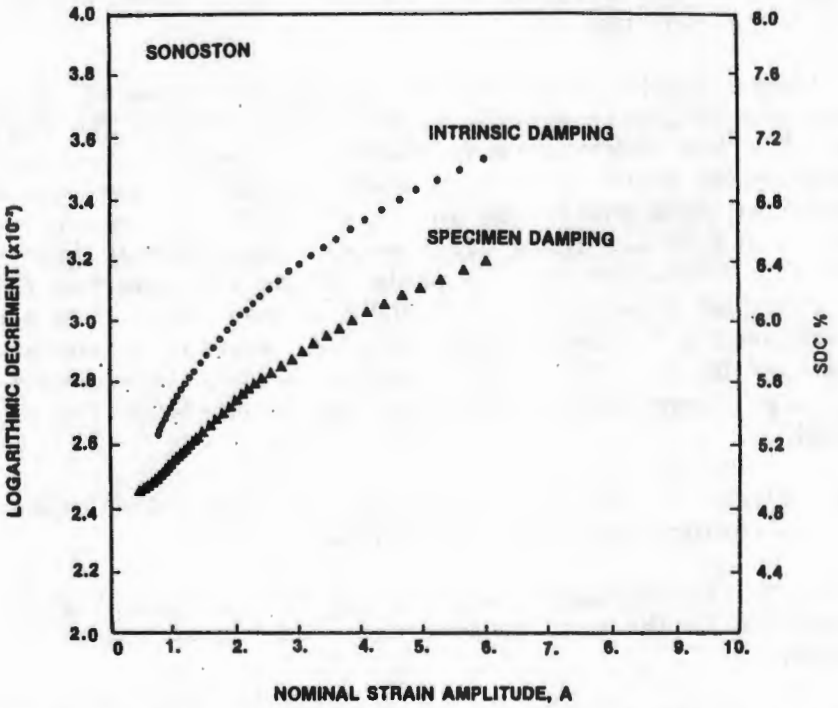

FIGURE 6: Comparison of measured specimen damping and calculated intrinsic damping for a sample of SONOSTON tested in a low-frequency flexure pendulum. The surface strain amplitude is equal to the nominal strain amplitude times 4.5×10^{-5}, while the logarithmic decrement is πQ^{-1} and specific damping capacity, (SDC) in percentage is $2\pi Q^{-1}/100$.

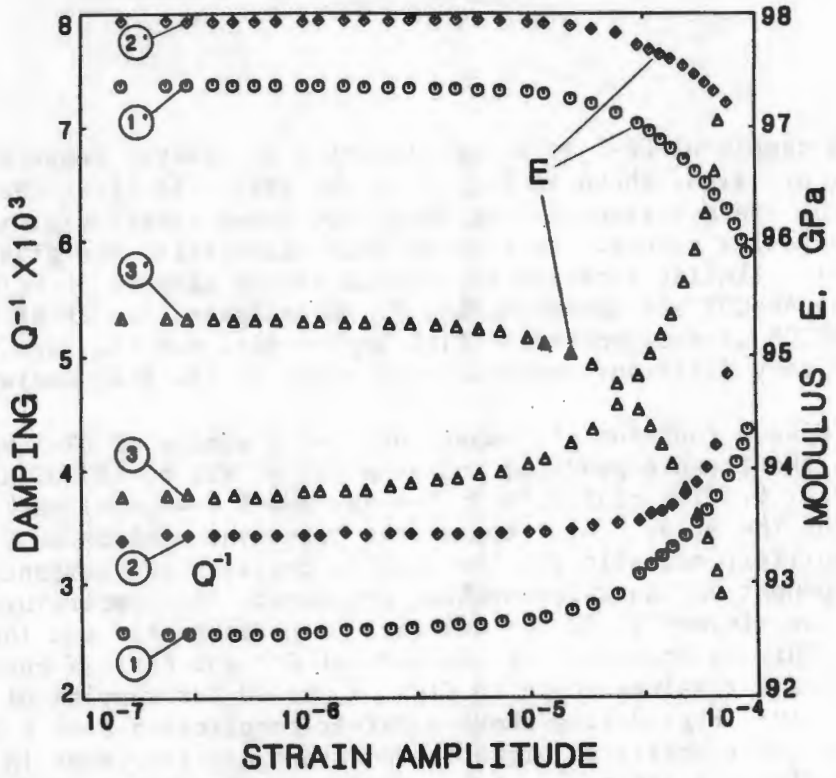

FIGURE 7: Damping and Young's modulus of samples of DR-1 and DR-4 as a function of strain amplitude at 20°C and 40 kHz: 1. as-received DR-4, 2. as-received DR-1, and 3. DR-4 after 2 h at 425°C and furnace cooling.

Fig. 8 is evidence of the fact that the thermally activated processes in the lower-temperature antiferromagnetic phase are shifted to the region of the phase change, but are inoperative in the higher-temperature paramagnetic phase. An important point to note in these results is the substantial differences in the Néel points and the forms of the Q^{-1} vs. T curves for samples of DR-1 and DR-4. These differences come entirely from microstructural differences between parts of the same casting that cooled at different rates. As shown in Figs. 7 and 8 respectively, the highest levels of damping achievable in the SONOSTON were not present in the as-received samples of either DR-4 or DR-1. Even higher damping levels were found at both low and high frequencies in samples heat-treated for 2 h at 425°C and furnace-cooled.

Combining the results of the flexure pendulum and APUCOT measurements revealed the following important conclusions:

1. The IF and E are strongly ε-dependent at both low and high frequencies at temperatures below the Néel temperature. At higher temperatures the IF is ε-independent.

2. At least one of the mechanisms is thermally activated, since the peak of Q^{-1} vs. T shifts to higher temperatures with higher frequencies. An unexpected feature of these results is that the overall peak height also increases with frequency (see Fig. 8).

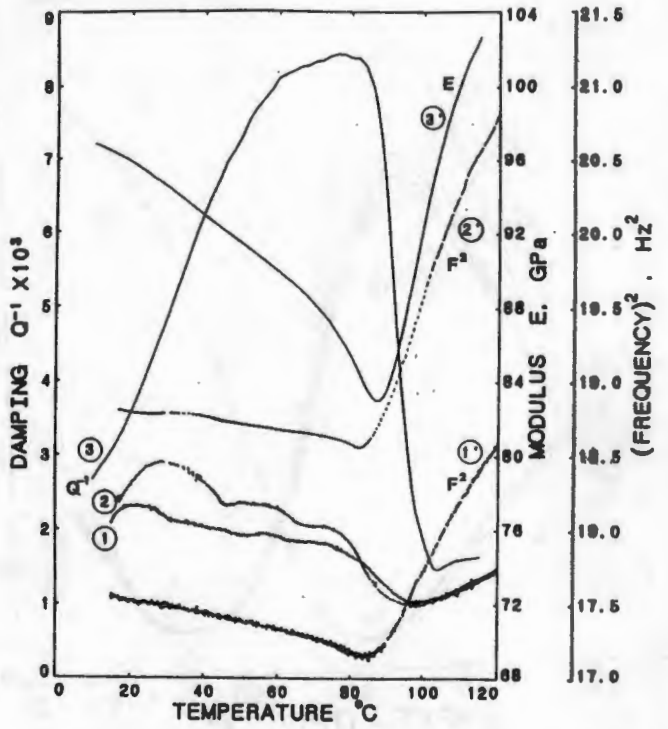

FIGURE 8: Damping and resonant frequency squared as a function of temperature for flexure pendulum tests on a sample of DR-1 before (1) and after (2) 2 h at 425°C. Damping and Young's modulus vs. temperature curves for a sample of DR-1 measured at 40 kHz (3). The strain amplitude in both types of test was 2×10^{-5}.

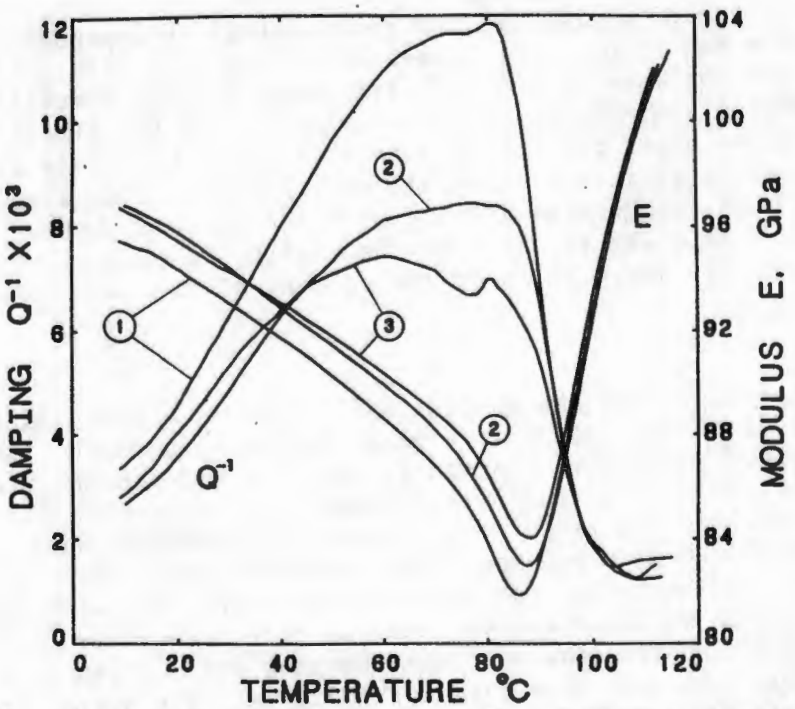

FIGURE 9: Q^{-1} and E vs. T curves for a sample of DR-1 measured at 40 kHz and different strain amplitudes: 1. $\varepsilon = 6 \times 10^{-5}$, 2. $\varepsilon = 2 \times 10^{-5}$, and 3. $\varepsilon = 2 \times 10^{-7}$.

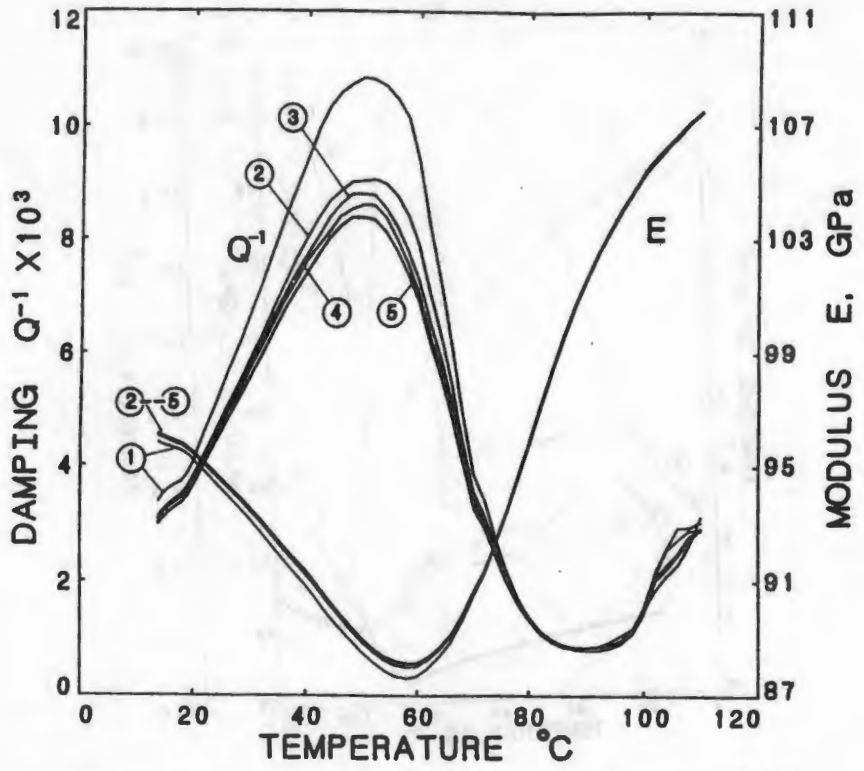

FIGURE 10: Q^{-1} and E vs. T curves for a sample of DR-4 measured at 40 kHz and different strain amplitudes: 1. $\varepsilon = 3.5 \times 10^{-5}$, 2. $\varepsilon = 1.2 \times 10^{-5}$ 3. $\varepsilon = 3.5 \times 10^{-6}$, 4. $\varepsilon = 1.2 \times 10^{-6}$, and 5. $\varepsilon = 3.5 \times 10^{-7}$.

The difficulties of characterizing the intrinsic ε dependence for each of the vibration modes used in our experiments, together with unknown mechanism that causes the increase in Q^{-1} with frequency for the thermally activated mechanism, make a semi-empirical description of the IF, similar to the description given above for the ZA-alloys, almost impossible for SONOSTON. Indeed, at present it is not clear if the same mechanisms are operative at both low and high frequencies in the antiferromagnetic phase. In addition, the variation from place to place in the casting is much too large to ignore in a semi-empirical description of the damping of the whole casting.

DISCUSSION

The characterization of the damping and stiffness properties of commercial HIDAMETS is a difficult and in some cases tedious procedure. We have outlined a method that works reasonably well for ε-dependent mechanisms and is not very different from the methods used to characterize viscoelastic materials. However, the majority of commercial HIDAMETS obtain their high-damping properties from ε-dependent mechanisms or mechanisms involving aspects of both dynamic and static hysteresis mechanisms that are highly sensitive to small microstructural changes. For such materials, it is a challenge to extract even the intrinsic damping for a given mode of vibration. This does not mean that such materials are not useful in practice, but it does mean that some other method of assessing the usefulness of the damping properties must be employed. A method that we have employed with some success involves the simple substitution of

materials for the component or structure involved, as mentioned in the introduction.

The ZA alloys are already used in hundreds of different applications and among these are several where the elevated damping of the alloy in question has proven to be of great benefit. For example, automobile engine mounts have been die-cast from ZA27 [12]. SONOSTON has been used to cast quiet submarine propellers.

CONCLUSIONS

The ZA alloys have elevated damping values at ambient temperatures compared with most of their competitors. This elevated damping is almost always a bonus in practical applications. At temperatures between 60 and 80°C, all of the ZA alloys become HIDAMETS in the sense that $Q^{-1} \geq 10^{-2}$. A characterization of this damping behaviour is given that allows the design engineer to estimate the damping of these alloys in flexure at useful values of thickness, temperature and frequency.

Properly heat-treated SONOSTON is also a HIDAMET at temperatures from about 0°C to the Néel point and high strain amplitudes ($\varepsilon > 10^{-4}$). But, because of the complexity of the mechanisms involved, it is not possible to present the damping behaviour in a simple manner (using a semi-empirical description) that will cover wide ranges of temperature, frequency or vibration strain amplitude.

ACKNOWLEDGEMENT

The research reported in this paper on the ZA alloys was funded by the International Lead Zinc Research Organization, Inc.

References

[1] Sahoo, M., Moore, V.E. and Weatherall, G., Canmet Report MRP/PMRL 84-61 (TR), 1984.

[2] Sprungmann, K.W. and Ritchie, I.G., "Instrumentation, Computer Software and Experimental Techniques Used in Low-Frequency Internal Friction Studies at WNRE," Atomic Energy of Canada Limited Report, AECL-6438 1980.

[3] Ritchie, I.G. and Pan, Z-L., "High Damping Metals and Alloys," Metallurgical Transactions A, 22A, 1991, in press.

[4] Rosinger, H.E., Ritchie, I.G. and Shillinglaw, A.J., "Improved Measurements of Elastic Properties at Acoustic Resonant Frequencies," Atomic Energy of Canada Limited Report, AECL-5114, 1976.

[5] Robinson, W.H. and Edgar, A., "The Piezoelectric method of Determining Mechanical Damping at 30 kHz," IEEE Transactions of Sonic and Ultrasonics SU-21, 1974, 98-105.

[6] Zener, C., Elasticity and Anelasticity of Metals, The University of Chicago Press, Chicago, Illinois, 1948.

[7] Nuttall, K., "The Damping Characteristics of a Superplastic Zn-Al Eutectoid Alloy," Journal of the Institute of Metals, 99, 1971, 266-270.

[8] Kawabi, K., and Kuwahara, K., "High Damping and Modulus Characteristics in a Superplastic Zn-Al Alloy," Journal de Physique, 42, 1981, C5-941-C5-946.

[9] Otani, T., Sakai, T., Hoshino, K. and Kurosawa, T., "Damping Capacity of Zn-Al Alloy Castings", Journal de Physique, 46, 1985, C10-417-C10-420.

[10] Ritchie, I.G., Pan, Z-L. and Goodwin, F.E., "Characterization of the Damping Properties of Die-Cast Zinc-Aluminum Alloys," Metallurgical Transactions A, 22A, 1991, in press.

[11] Ritchie, I.G., Schmidt, H.K. and Sprungmann, K.W., "Non-Linear Internal Friction from Flexure Pendulum Measurements," Journal de Physique, 46, 1985, C10-791-C10-794.

[12] Lyon, R. and Spillane, A.F., "The Development of ZA-27 Engine Mounts by Austin Rover", Proc. SAE Conf., Detroit, Michigan, February 1988.